

Research Article

Motion Capture Technology and Its Applications in Film and Television Animation

Yong Guo ¹ and Chan Zhong²

¹College of Art and Design, Hubei Engineering University, Xiaogan, Hubei 432100, China

²Termax Fastener Systems (Suzhou) Co., Ltd., Kunshan, Jiangsu 215300, China

Correspondence should be addressed to Yong Guo; wylgl@hbeu.edu.cn

Received 30 May 2022; Revised 5 July 2022; Accepted 29 July 2022; Published 25 August 2022

Academic Editor: Qiangyi Li

Copyright © 2022 Yong Guo and Chan Zhong. This is an open access article distributed under the Creative Commons Attribution License, which permits unrestricted use, distribution, and reproduction in any medium, provided the original work is properly cited.

In order to improve the production effect of film and television animation, this paper combines motion capture technology to construct a film and television animation production system and proposes a simple correction method to eliminate the instability of animation frames. This method suppresses the occurrence of instability by introducing additional viscosity corresponding to shear waves in the vicinity of strong shock waves. Furthermore, this paper constructs two Riemannian solvers, HLLC and HLLE, to study the stability of numerical carbuncle problems. In addition, this paper builds a film and television animation production system based on motion capture technology. Through the verification of motion capture and animation production effects, it can be seen that the film and television animation system based on motion capture technology proposed in this paper can effectively promote the improvement of the animation production effect.

1. Introduction

The animation production process must first be built based on the sub scene script, so the writing of the subscene script is very important. Moreover, a cartoon consists of several paragraphs, each paragraph consists of several scenes, each scene contains several plot segments, and each plot segment is composed of several shots [1]. In short, a film is made up of shots. The subshot script is to process the story into shots and formulate the time length of the shots, the movement methods of the shots, the content of the shots, and the arrangement relationship between the shots in detail according to the montage thinking. It is roughly classified into storyboard according to the dialogue of the characters, storyboard according to the movement relationship of the characters, storyboard according to the turning point of the characters' emotions, storyboard according to the psychological changes of the objects, storyboard according to the perspective transformation, storyboard according to the causal chain, and other methods [2]. In the storyboard stage, 3D computer animation is fundamentally different from 2D

hand-drawn animation. 3D animations can be produced using storyboards, which greatly reduces the workload in the preparatory stage. In particular, the virtual camera not only simplifies the storyboard work but also allows flexible framing, free composition changes, and random switching of shots, which makes the compositional relationship and performance of the lens images more optional [3].

Synthesis technology is also a general technology in two-dimensional movements. The most noteworthy thing in synthesis technology is the production of movements. Action production in 3D animation is a kind of composite production. With the upgrade of production software, more synthesis tools are also provided [4].

Traditional animation design is often restricted by realistic conditions, such as changes in objects, movement of objects, etc. However, 3D animation production technology can realize flexible animation design and produce arbitrary changing effects. One is the fictional movement [5]. The application of 3D animation technology can virtualize movement in the real environment [6]. The second is continuous shooting. 3D animation production technology

can be applied to achieve continuous shooting, from the macroworld to the microworld naturally, to achieve uninterrupted shooting, and it can also naturally enter the macro world from the microworld [7]. For example, it can take a macro shot of a city, and then enter the micro-internal world, so that the shots can be kept coherent and will not cause the sense of camera switching. The third is the variable object. Three-dimensional animation technology can provide two deformation methods. One is the deformation of the three-dimensional shape and the other is the deformation of the image level. In this way, the artistic expression effect of metaphor can be achieved, resulting in direct interpretation, and at the same time strengthening the persuasive effect [8].

The texture of objects is one of the important contents of animation performance. 3D animation technology can enrich texture performance and strengthen artistic effects. In general, the texture and color of the material are determined by the properties of the surface, such as the brightness, reflection, and absorption of light on the surface of the material. These properties often depend on the material composed of the body. 3D animation production technology provides a variety of materials. The library can achieve the largest range of material coverage, thus enriching the texture performance [9]. Lighting is one of the important factors affecting the texture of the material. The 3D animation production technology will realize the optimization of the lighting design. By flexibly selecting the type and type of the light, and freely changing the brightness and darkness of the light, moving the position of the light, using Light reflection, shadow effects, etc. [10].

Bone and skinning are used for animation binding. The bones are connected through joint chains. Bone joints are added at the positions that need to be moved and the model is associated with the bones through skinning. We adjust the distribution of the weight of the bone to the model through the skin weight drawing to meet the requirements of animation. Animation production is the most important part of 3D animation production. The key to animation production lies in animation adjustment. Character movements and expressions are the keys to plot development and character characteristics [11]. The effect of the cartoon depends on the action of the character, and the action of the character is often the most tedious process in production. The mid-production of animation is the result of the joint efforts of all the production staff [12].

Polygon modeling technology is one of the most commonly used modeling methods in modeling technology. Polygon refers to the polygon meshes composed of polygonal meshes, and the model is composed of polygonal meshes [13]. The polygonal patch in digital model modeling requires a four-sided mesh structure. For non-four-sided surfaces, it is necessary to modify them into four-sided surfaces, and a reasonable topology model can meet the requirements of animation production. Polygon modeling is easier to operate. For the modification of polygons, the digital model provides a wealth of modification command operations, which is very convenient to use. Polygon modeling in modeling technology is suitable for various

morphological models such as buildings, game characters, and animation characters. It is the most commonly used in modeling production technology and is the main means of 3D model construction [14]. Subdivision surface modeling can simplify the production process of complex objects. It takes into account both polygon modeling and NURBS surface modeling technology. It is a comprehensive modeling technology that can be switched between surfaces and polygon meshes through conversion, which combines the common features of both. It is usually used to build props in modeling, which can greatly improve the modeling speed and shorten the animation production cycle [15]. Lighting and material technology are very important in digital models. Lights can simulate indoor and outdoor lighting of lights. The use of lights can express the time dimension of the animation scene environment, such as morning, sunset, sunny, thunderstorm, and other natural environments. Through the use of lighting, the development and ups and downs of the story and the character of the characters can be expressed [16]. For example, different angles of lighting can clearly convey character characters such as heroes and demons, and different color temperatures of lighting can also express environmental atmospheres such as the joy of festivals and the fear of disasters. There are six basic types of lights in the digital model: ambient light, directional light, point light, spot light, area light, and volume light, each of which has its own characteristics and different uses [17]. If there is only a good lighting atmosphere, and there are no complex and changing models and materials, the final rendered picture will not be vivid and exciting, so the model, lighting, material, and animation complement each other, and each link directly affects the final effect. The materials and textures of the digital model can simulate any material effects in the natural environment such as metal, glass, plastic, cloth, wood, and stone. The digital model provides a variety of surface shaders to simulate material effects with and without highlights [18]. The lighting and materials of the digital model are an important part of the animation production of the digital model. Exquisite textures, realistic textures, and reasonable materials can express the model incisively and vividly. A large part of the realistic expression of virtual effects is created by excellent lighting engineers and materials. It is determined by the level of the teacher [19]. Animation technology. The digital model has a variety of animation production technology methods, such as path animation, keyframe animation, expression animation, deformation animation, driving animation, particle animation, and other animation forms. The digital model includes advanced animation production tools such as deformers, constraints, nonlinear animation editing systems, bones, and skin systems, including skeletal systems, IK spline handles, skin weight drawing and distribution, and other animation production techniques [20]. Digital model animation also produces various character expression animations through fusion deformation technology. The skeletal system of the digital model is very powerful, and the skeletal control system is to assemble these animation objects before animating the characters and objects of the scene. The whole process of creating bones, adding control systems to bones,

skinning bones, and adding deformations and constraints to characters is called rigging, also known as character setup. Create character animation through the skeleton system, bind bones to create controllers, and after skinning, you can control the deformation of the model by rotating the bones. In digital model character animation, the animator does not directly use the most primitive bone chain to control the character animation but adds a series of control systems to the bone inscription, such as the IK system, driving keyframes, attribute association, constraints, etc., to facilitate production animation. In the process of skinning, some additional control systems may be added, such as flexor system, muscle deformation system, and associative deformation. A completed character animation control system [21].

This paper combines motion capture technology to build a film and television animation production system to improve the production effect of modern film and television animation.

2. Digital Motion Capture Technology

2.1. Numerical Dissipative Study of Godunov-Type Schemes. There is a close relationship between the numerical viscosity of the animation frame capture method and its numerical animation frame stability, and this part will focus on this problem in detail. In order to facilitate subsequent analysis, here is a brief review of two classic HLL-type Riemann solvers: HLLC format and HLLC format.

It is well known that animation frame capture formats that can accurately capture contact discontinuities and shear waves are prone to frame instability problems. However, very little work has focused on investigating which numerical viscosity is really effective in suppressing animation frame instability.

Considering the Riemann problem of the system of equations, $x_{i+1/2}$ can be expressed as follows:

$$\omega_{i+1/2} \left[\frac{(x - x_{i+1/2})}{(t - t^n)} \right],$$

$$\omega_{i+1/2} \left(\frac{x'}{t} \right) = \begin{cases} U_i & \frac{x'}{t} < S_L, \\ U_{i+1/2} & \frac{S_L < x'}{t} < S_R, \\ U_{i+1} & \frac{x'}{t} > S_R. \end{cases} \quad (1)$$

Among them, $x' = x - x_{i+1/2}$, S_L and S_R represent the minimum and maximum wave velocities at interface $x_{i+1/2}$. Furthermore, for ease of exposition, we assume $t^n = 0$ here.

The approximate solution of the Riemann problem in the HLLC scheme only includes the minimum and maximum wave velocities, while ignoring the intermediate wave velocities, so the contact discontinuity and shear waves cannot be distinguished. In order to reduce the numerical viscosity of the HLLC scheme, Einfeldt proposed a method to modify

the Riemann solution by adding an inverse dissipation term. According to Einfeldt's method, only the inverse dissipation term corresponding to the entropy wave is first considered here. Therefore, the average state $U_{i+1/2}$ in the solution of the Riemann problem can be corrected as follows:

$$\omega_{\text{HLLC}} = \begin{cases} U_i, & \frac{x'}{t} < S_L, \\ U_{i+1/2} + (x - \hat{q}_{i+1/2} t) \hat{\delta}_{2,i+1/2} \hat{\alpha}_{2,i+1/2} \hat{R}_{2,i+1/2}, & \frac{S_L < x'}{t} < S_R, \\ U_{i+1}, & \frac{x'}{t} > S_R, \end{cases} \quad (2)$$

$$F_{\text{HLLC}} = \frac{S_R^+ F(U_L) - S_L^- F(U_R)}{S_R^+ - S_L^-} + \frac{S_L^- S_R^+}{S_R^+ - S_L^-} (U_R - U_L - \hat{\delta}_2 \hat{\alpha}_2 \hat{R}_2).$$

Similarly, if only the inverse dissipation term corresponding to the shear wave is added, the solution to the Riemann problem can be expressed as [22]:

$$\omega_{\text{HLLS}} = \begin{cases} U_i, & \frac{x'}{t} < S_L, \\ U_{i+1/2} + (x - \hat{q}_{i+1/2} t) \hat{\delta}_{3,i+1/2} \hat{\alpha}_{3,i+1/2} \hat{R}_{3,i+1/2}, & \frac{S_L < x'}{t} < S_R, \\ U_{i+1}, & \frac{x'}{t} > S_R. \end{cases} \quad (3)$$

The corresponding Riemann solver HLLS can be expressed as follows:

$$F_{\text{HLLS}} = \frac{S_R^+ F(U_L) - S_L^- F(U_R)}{S_R^+ - S_L^-} + \frac{S_L^- S_R^+}{S_R^+ - S_L^-} (U_R - U_L - \hat{\delta}_3 \hat{\alpha}_3 \hat{R}_3). \quad (4)$$

In this paper, two Riemannian solvers HLLC and HLLS are constructed. In order to clarify their dissipation mechanism, these two formats can be expressed as a unified form such as formula together with the classical HLLC format and HLLS format. It can be observed that the only difference between the four formats is the definition of the inverse dissipation coefficient. This paper adopts the flux form that shows the numerical viscosity, namely:

$$F_{1/2} = \frac{1}{2} (F_L + F_R) + D_{1/2}, \quad (5)$$

$$D_{1/2} = \frac{S_R^+ + S_L^-}{2(S_R^+ - S_L^-)} (F_L - F_R) + \frac{S_L^- S_R^+}{S_R^+ - S_L^-} \cdot (U_R - U_L - \hat{\delta}_2 \hat{\alpha}_2 \hat{R}_2 - \hat{\delta}_3 \hat{\alpha}_3 \hat{R}_3). \quad (6)$$

Here, we consider two special and important cases. One is the steady entropy wave problem, and the other is the steady shear wave problem. Figure 1 shows the schematic diagram of the two problems.

By giving an initial density discontinuity, a simple entropy wave can be obtained, namely:

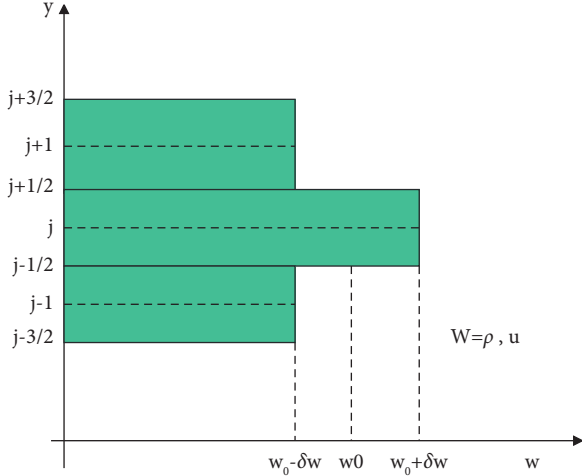


FIGURE 1: Schematic diagram of steady-state discontinuity.

$$(\rho, u, v, p)_{I,K} = \begin{cases} (\rho_0 + \delta\rho, u_0, 0, p_0), & K = J, \\ (\rho_0 - \delta\rho, u_0, 0, p_0), & K = J + 1. \end{cases} \quad (7)$$

Among them, (ρ_0, u_0, v_0, p_0) denotes a given uniform initial condition. Under this condition, the corresponding viscosity term can be expressed as follows:

$$\mathbf{D}_{1/2}|_1 = -\frac{2S_L S_R}{S_R - S_L} [(1 - \widehat{\delta}_2) \cdot \delta\rho],$$

$$\widehat{\delta}_2 = 1,$$

$$(\rho, u, v, p)_{I,K} = \begin{cases} (\rho_0, u_0 + \delta u, 0, p_0), & K = J, \\ (\rho_0, u_0 - \delta u, 0, p_0), & K = J + 1, \end{cases}$$

$$\mathbf{D}_{1/2}|_2 = -\frac{2S_L S_R}{S_R - S_L} [(1 - \widehat{\delta}_3) \rho_0 \cdot \delta u],$$

$$\widehat{\delta}_3 = 1,$$

$$\rho_J^n = \rho_0 + \delta\rho^n, p_J^n = p_0 + \delta p^n, u_J^n = u_0 + \delta u^n, v_J^n = v_0,$$

$$\rho_{J\pm 1}^n = \rho_0 - \delta\rho^n,$$

$$p_{J\pm 1}^n = p_0 - \delta p^n,$$

$$u_{J\pm 1}^n = u_0 - \delta u^n,$$

$$v_{J\pm 1}^n = v_0.$$

(8)

This paper uses the linear perturbation analysis method to illustrate how the four Godunov-type schemes defined by formulas (5) and (6) and Table 1 suppress small perturbations.

With the proper inverse dissipation term, the HLLEM format can accurately capture entropy waves and shear waves.

TABLE 1: Definition of four HLL type formats.

	HLLEM	HLLEC	HLLES	HLL
$\widehat{\delta}_2$	$\widehat{a}/(\widehat{a} + \widehat{q})$	$\widehat{a}/(\widehat{a} + \widehat{q})$	0	0
$\widehat{\delta}_3$	$\widehat{a}/(\widehat{a} + \widehat{q})$	0	$\widehat{a}/(\widehat{a} + \widehat{q})$	0

2.2. Numerical Test Setup. Due to the strong nonlinearity of numerical animation frame instability, especially the complexity of multidimensional instability, there is still a lack of effective theoretical analysis methods and it is difficult to study its mechanism from a theoretical level. Therefore, numerical experiments have become one of the reliable ways to study the stability of animation frame capture methods. This paper focuses on the stability study of numerical carbuncle problems. This problem usually occurs in the numerical simulation of flow around a hypersonic blunt body, especially since the numerical format used has the properties of low dissipation and high resolution. In order to facilitate the analysis, this paper selects a standard steady-state normal animation frame problem in a two-dimensional area as a research example. If the numerical method produces instability in this steady-state animation frame study, it will produce numerical ‘‘carbuncles’’ in the flow around a blunt body. Therefore, based on this problem, this paper conducts an in-depth analysis of the numerical ‘‘carbuncle’’ phenomenon, explores its mechanism, and proposes corresponding cure methods. To facilitate further discussion later, this subsection briefly describes the experimental setup for this example and presents the frame instability characteristics of a typical numerical animation of a low-dissipation Riemann solver.

As shown in Figure 2, the calculation area consists of 50×25 uniform grids. The flow field is initialized as follows:

$$U_L = \begin{pmatrix} 1 \\ 1 \\ 0 \\ \frac{1}{\gamma(\gamma-1)M_0^2} + \frac{1}{2} \end{pmatrix}, \quad (9)$$

$$U_R = \begin{pmatrix} f(M_0) \\ 1 \\ 0 \\ \frac{g(M_0)}{\gamma(\gamma-1)M_0^2} + \frac{1}{2f(M_0)} \end{pmatrix}.$$

In the formula, the functions $f(M_0)$ and $g(M_0)$ can be expressed as follows:

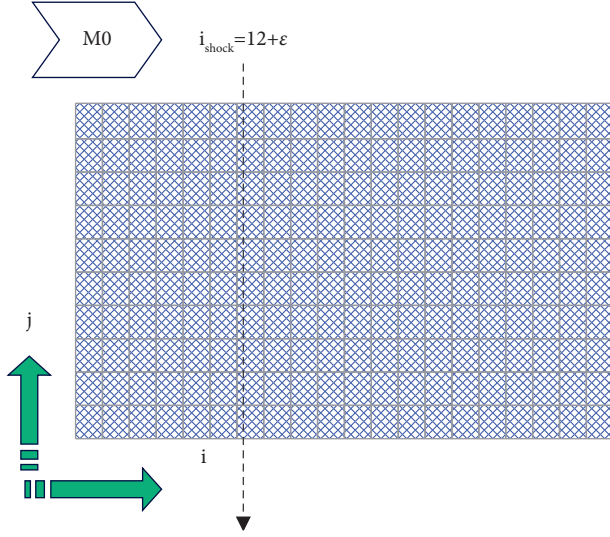


FIGURE 2: Computational grid and initial conditions for the quasi-one-dimensional (1.5D) steady-state animation frame problem.

$$f(M_0) = \left(\frac{2}{(\gamma + 1)M_0^2} + \frac{\gamma - 1}{\gamma + 1} \right)^{-1}, \quad (10)$$

$$g(M_0) = \frac{2\gamma M_0^2}{\gamma + 1} - \frac{\gamma - 1}{\gamma + 1}.$$

Among them, M_0 and γ represent the incoming Mach number and the gas-specific heat ratio, respectively. In this problem, the incoming flow boundary condition is set as free incoming flow. In order to keep the mass flow in the computational domain constant and to fix the animation frame at the same position, the mass flow in the virtual grid is specified as follows:

$$(\rho u)_{i_{\max}+1,j} = (\rho u)_0 = 1. \quad (11)$$

Other variables can be obtained by extrapolation. The state quantity in the animation frame is assumed to be on the Yugon line, and this intermediate state quantity ($M: i = 13$) can be expressed as follows:

$$\begin{aligned} \rho_M &= (1 - \alpha_p)\rho_L + \alpha_p\rho_R, \\ u_M &= (1 - \alpha_u)u_L + \alpha_u u_R, \\ p_M &= (1 - \alpha_p)p_L + \alpha_p p_R. \end{aligned} \quad (12)$$

Among them,

$$\begin{aligned} \alpha_p &= \varepsilon, \\ \alpha_u &= 1 - (1 - \varepsilon) \left(1 + \varepsilon \frac{M_0^2 - 1}{1 + (\gamma - 1)M_0^2/2} \right)^{-1/2}, \\ &\left(1 + \varepsilon \frac{M_0^2 - 1}{1 - 2\gamma M_0^2/(\gamma - 1)} \right)^{-1/2}, \\ \alpha_p &= \varepsilon \left(1 + (1 - \varepsilon) \frac{\gamma + 1}{\gamma - 1} \frac{M_0^2 - 1}{M_0^2} \right)^{-1/2}. \end{aligned} \quad (13)$$

In the formula, $\varepsilon = 0.0, \dots, 0.9$ represents the discrete weighted average. Here, it represents the initial state within the grid in the middle of the animation frame, referred to herein as the animation frame position. In the case of different incoming Mach numbers and animation frame positions, in this paper, the HLL-type format defined above is used to calculate the quasi-one-dimensional (1.5D) normal animation frame problem and its corresponding one-dimensional problem (1D), that is, only one layer of grid is used in the direction parallel to the animation frame.

Both theoretical analysis and numerical experimental studies have shown that a Riemann solver capable of capturing stationary animation frames with a single interior point is not always stable. Like the Godunov and the Roe formats, the HLL and HLLM formats for formula calculation of wave velocity are used to give a numerical animation frame structure containing an intermediate state point. In the case of strong animation frames and different animation frame positions, these formats suffer from instability of one-dimensional numerical animation frames, that is, one-dimensional “carbuncle” problems. All HLL-type formats produce unstable results at animation frame positions $\varepsilon = 0.0 \sim 0.3$. In the one-dimensional case, the HLLC format degenerates to the HLLM format, and the HLLS format degenerates to the HLL format. Compared with the HLLM scheme, the approximate solution of the HLLC scheme to the Riemann problem ignores the contact wave, thus introducing excessive numerical viscosity to the contact discontinuity. However, the HLLC format, like the HLLM format, still suffers from 1D animation frame instability at certain animation frame positions. The numerical viscosity corresponding to the contact wave cannot effectively suppress the instability of one-dimensional numerical animation frames, that is, the one-dimensional “carbuncle” problem.

Figure 3 shows the results of the steady-state animation frame calculated at the stable animation frame position in the HLLM format. However, for some unstable animation frame positions, the calculation results do not converge to a steady state. Figure 4 shows the essential characteristics of the one-dimensional “carbuncle” phenomenon. In the unstable case, intermediate states within the animation frame structure oscillate and enter an approximate limit cycle. The HLLC format gives similar results and is not shown for clarity.

It is worth noting that Ismail and Zaide use Roe format as an example to illustrate the unstable characteristics of the one-dimensional “carbuncles” problem. For Godunov-type formats, especially those with minimal dissipation at animation frames, the one-dimensional “carbuncles” problem is a common numerical anomaly.

3. Motion Capture Technology and Its Applications in Film and Television Animation

In the motion capture system, the production process of film and television animation performance is shown in Figure 5.

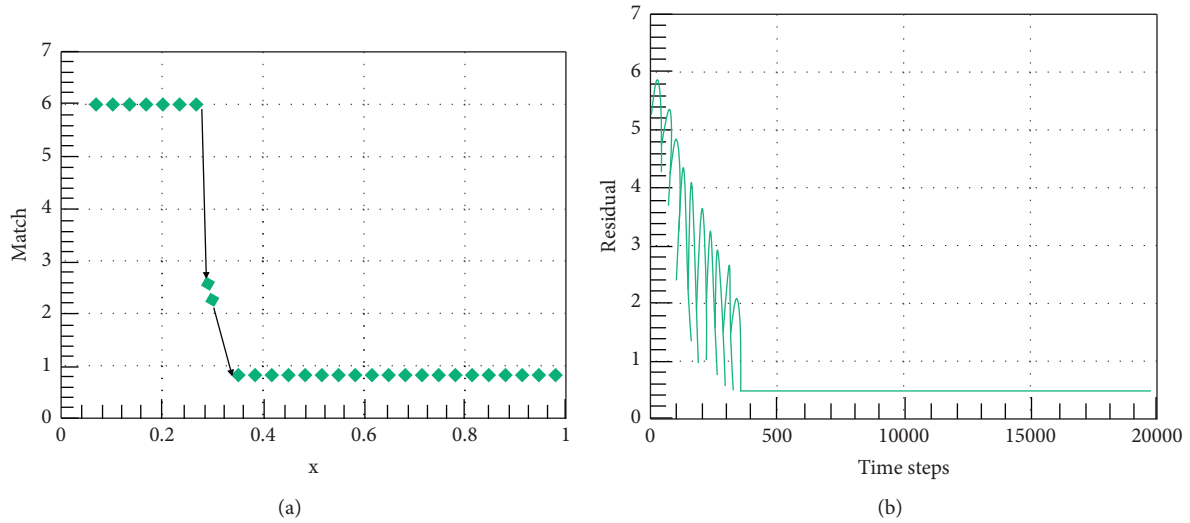


FIGURE 3: Animation frame profile calculated in HLEM format ($M_0 = 6.0$, $\varepsilon = 0.5$). (a) Mach number distribution curve. (b) Residual value convergence curve.

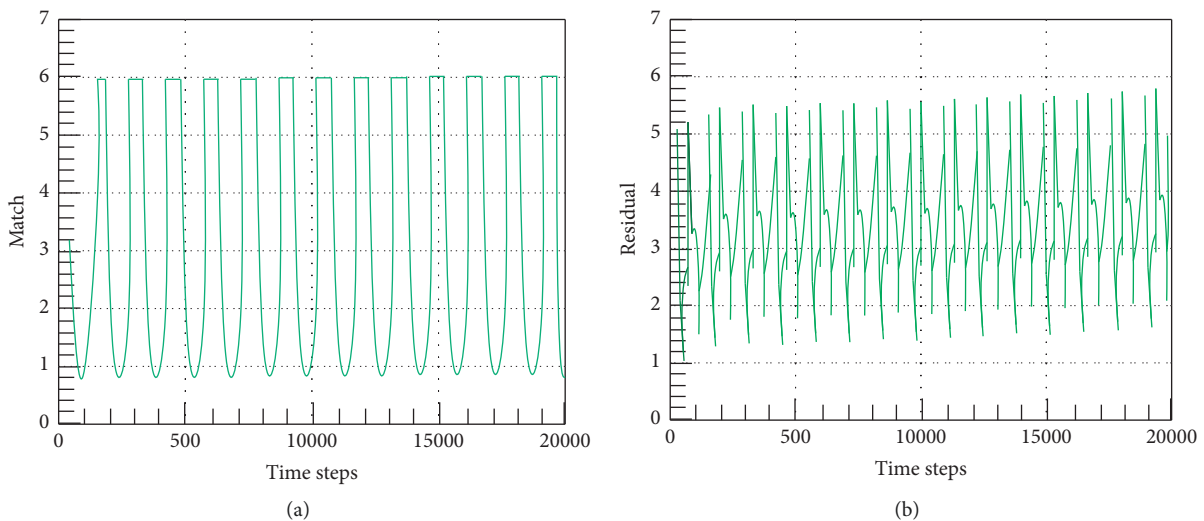


FIGURE 4: One-dimensional “carbuncle” problem calculated in HLEM format ($M_0 = 6.0$, $\varepsilon = 0.3$. For clarity, only the results before 20000 time steps are shown in the figure). (a) Mach number. (b) Residual value convergence curve.

The first is to use 3D modeling software to carry out digital modeling design according to the script design, so as to design the required animation model. Second, when the performer is performing, the video capture card is used to capture the action, so as to obtain the data of the performer, and then drive the animation model of the computer, thus generating the animation sequence. In the real film and television animation production process, the data captured by motion are often difficult to provide continuous control of the entire motion. In addition, motion capture is also a high-cost and time-consuming technology, and it is impossible for the performer to perform exactly as the artist imagined, so the data that can be used are only segments. Therefore, the animator has an important responsibility throughout the production process to match the captured data with the designed plot and synthesize it. After

completing the preliminary processing work, model driving can be carried out. After that, with the help of the model created by the 3D modeling software used at the beginning, the animation is synthesized to form the final film and television animation work.

The essence of the data processing process is to use a certain algorithm to filter out the noisy data, repair the missing data, and identify the topological structure relationship between the scattered points in space so that they become ordered points. In this way, attribute information is added to each point, and finally, it becomes complete and useable human motion data, which can be converted into a general motion data format. The scattered data processing algorithm based on template rigid structure matching proposed in this paper completes the data processing task through a series of processing procedures. The data

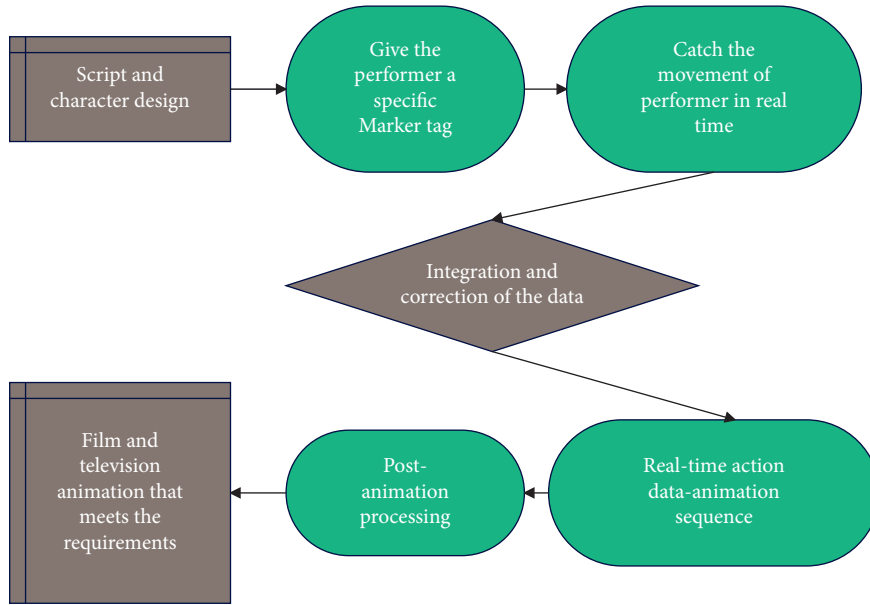


FIGURE 5: The production process of film and television animation in the motion capture system.

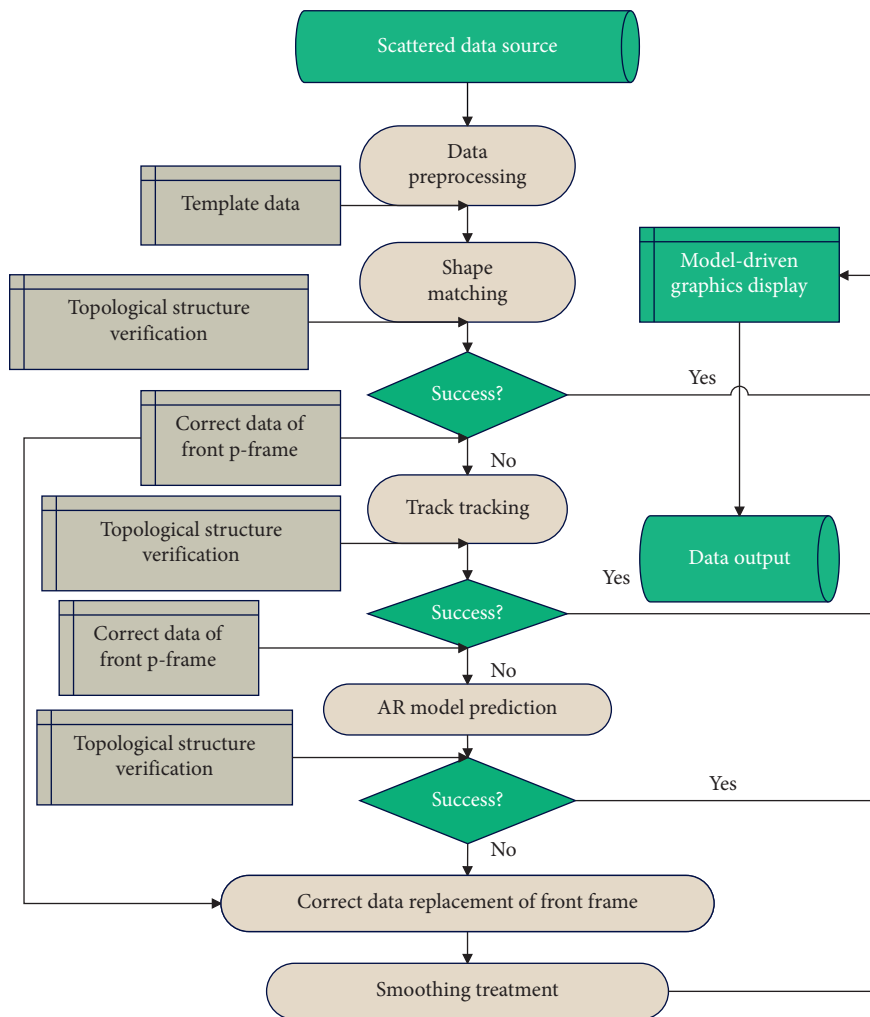


FIGURE 6: Flowchart of the scattered data processing algorithm.

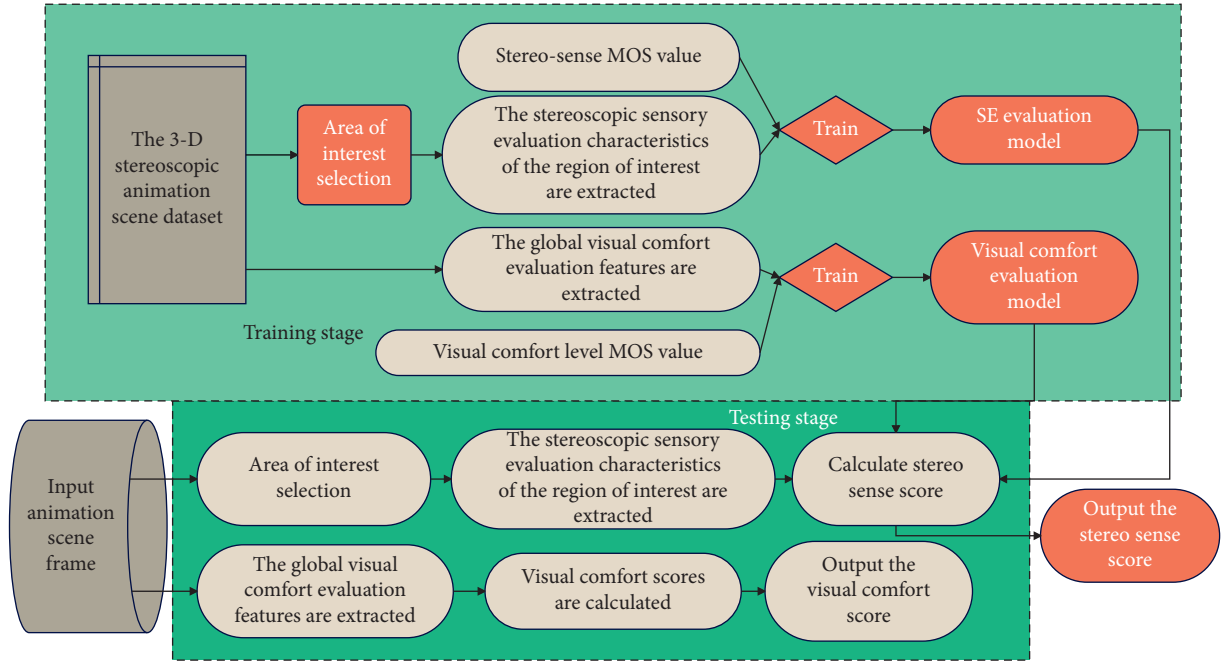


FIGURE 7: The overall process of evaluation for the reproduction of 3D stereo animation realized by the evaluation model in this paper.

processing algorithm flow is shown in Figure 6. The main steps include point cluster clustering, rigid structure matching, motion trajectory tracking, topology verification, and AR model-based missing point prediction.

The algorithm in this paper mainly includes two stages: training and testing. The algorithm flow framework is shown in Figure 7. In the training phase, we first construct a 3D stereo image dataset for preproduction animation scenes. Afterward, subjective experiments are performed on the stereoscopic image pairs of scene frames in the dataset to obtain the MOS values (the “average evaluation score”) of visual comfort and stereoscopic perception, respectively. For the entire scene, we extract the global visual comfort evaluation features, use the SVR method to establish the mapping relationship between the global visual comfort evaluation feature parameters and the visual comfort score, and obtain the visual comfort evaluation model. After that, we select the region of interest, extract the stereoscopic evaluation features of the region of interest, use the SVR method to establish the relationship between the stereoscopic evaluation features of the region of interest and the stereoscopic score, and obtain a stereoscopic evaluation model. In the testing phase, by extracting the global visual comfort evaluation features of the input stereo image pair and the stereoscopic evaluation features of the region of interest and using the evaluation model obtained by training, the visual comfort score and the stereoscopic score of the output animation scene are finally calculated.

The system structure is improved by improving the algorithm, the system is verified, and the system structure and performance are quantified, as shown in Figures 8 and 9.

Through the verification of motion capture and animation production effect, it can be seen that the film and

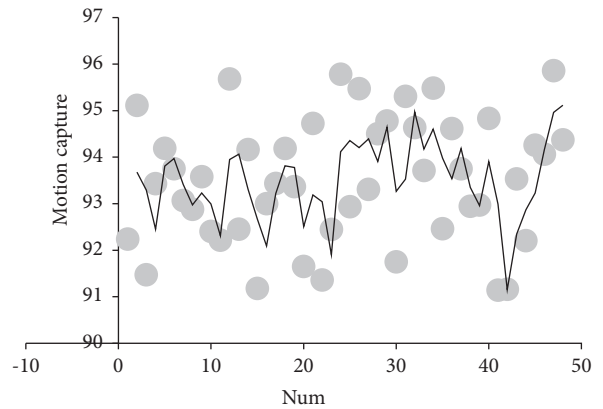


FIGURE 8: Motion capture effect. Statistical analysis is carried out on the practical effect of the system in this paper, and the quantitative processing method is used to obtain it.

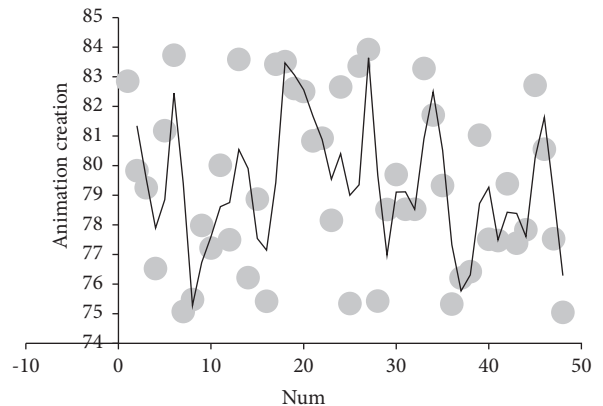


FIGURE 9: The effect of animation production.

television animation system based on motion capture technology proposed in this paper can effectively promote the improvement of the animation production effect.

4. Conclusion

Motion capture technology plays a very important role in the production of film and television animation and the two complement each other. It can also be said that motion capture technology is also a technology that emerged and developed on the basis of the huge demand for film and television animation production. With the advancement of science and technology, the application of this technology is more extensive, involving many fields such as film and television, multimedia, and games. It is precisely because of the application of this technology that the workload of traditional manual editing in the animation creation process is reduced. This paper combines motion capture technology to construct a film and television animation production system to improve the production effect of modern film and television animation. Through the verification of motion capture and animation production effect, it can be seen that the film and television animation system based on motion capture technology proposed in this paper can effectively promote the improvement of the animation production effect.

Data Availability

The labeled dataset used to support the findings of this study is available from the corresponding author upon request.

Conflicts of Interest

The authors declare that they have no conflicts of interest.

Acknowledgments

This study was sponsored by Phased Achievements of the Provincial First-Class Course “Two-Dimensional Animation Design”.

References

- [1] J. Steffens, “The influence of film music on moral judgments of movie scenes and felt emotions,” *Psychology of Music*, vol. 48, no. 1, pp. 3–17, 2020.
- [2] G. Schalk, C. Kapeller, C. Guger et al., “Facephenes and rainbows: causal evidence for functional and anatomical specificity of face and color processing in the human brain,” *Proceedings of the National Academy of Sciences*, vol. 114, no. 46, pp. 12285–12290, 2017.
- [3] S. Han, B. Liu, R. Wang, Y. Ye, C. D. Twigg, and K. Kin, “Online optical marker-based hand tracking with deep labels,” *ACM Transactions on Graphics*, vol. 37, no. 4, pp. 1–10, 2018.
- [4] D. Stawarczyk, M. A. Bezdek, and J. M. Zacks, “Event representations and predictive processing: the role of the midline default network core,” *Topics in Cognitive Science*, vol. 13, no. 1, pp. 164–186, 2021.
- [5] A. G. Sares, N. E. V. Foster, K. Allen, and K. L. Hyde, “Pitch and time processing in speech and tones: the effects of musical training and attention,” *Journal of Speech, Language, and Hearing Research*, vol. 61, no. 3, pp. 496–509, 2018.
- [6] A. K. Fishell, T. M. Burns-Yocum, K. M. Bergonzi, A. T. Eggebrecht, and J. P. Culver, “Mapping brain function during naturalistic viewing using high-density diffuse optical tomography,” *Scientific Reports*, vol. 9, no. 1, pp. 11115–11211, 2019.
- [7] E. Peters and C. Muñoz, “Introduction to special issue Language learning from multimodal input,” *Studies in Second Language Acquisition*, vol. 42, no. 3, pp. 489–497, 2020.
- [8] C. Li, Z. Wang, Y. Lu, X. Liu, and L. Wang, “Conformation-based signal transfer and processing at the single-molecule level,” *Nature Nanotechnology*, vol. 12, no. 11, pp. 1071–1076, 2017.
- [9] N. Molinaro and M. Lizarazu, “Delta (but not theta)-band cortical entrainment involves speech-specific processing,” *European Journal of Neuroscience*, vol. 48, no. 7, pp. 2642–2650, 2018.
- [10] Y. Deldjoo, M. F. Dacrema, M. G. Constantin et al., “Movie genome: alleviating new item cold start in movie recommendation,” *User Modeling and User-Adapted Interaction*, vol. 29, no. 2, pp. 291–343, 2019.
- [11] R. Piryani, V. Gupta, and V. K. Singh, “Movie Prism: a novel system for aspect level sentiment profiling of movies,” *Journal of Intelligent and Fuzzy Systems*, vol. 32, no. 5, pp. 3297–3311, 2017.
- [12] T. Alexopoulou, M. Michel, A. Murakami, and D. Meurers, “Task effects on linguistic complexity and accuracy: a large-scale learner corpus analysis employing natural language processing techniques,” *Language Learning*, vol. 67, no. S1, pp. 180–208, 2017.
- [13] S. De Jans, D. Van de Sompel, L. Hudders, and V. Cauberghe, “Advertising targeting young children: an overview of 10 years of research (2006–2016),” *International Journal of Advertising*, vol. 38, no. 2, pp. 173–206, 2019.
- [14] F. M. Schneider, “Measuring subjective movie evaluation criteria: conceptual foundation, construction, and validation of the SMEC scales,” *Communication Methods and Measures*, vol. 11, no. 1, pp. 49–75, 2017.
- [15] M. A. Mizher, M. C. Ang, A. A. Mazhar, and M. A. Mizher, “A review of video falsifying techniques and video forgery detection techniques,” *International Journal of Electronic Security and Digital Forensics*, vol. 9, no. 3, pp. 191–208, 2017.
- [16] J. T. Fisher, J. R. Keene, R. Huskey, and R. Weber, “The limited capacity model of motivated mediated message processing: taking stock of the past,” *Annals of the International Communication Association*, vol. 42, no. 4, pp. 270–290, 2018.
- [17] V. Grech, “The application of the Mayer multimedia learning theory to medical PowerPoint slide show presentations,” *Journal of Visual Communication in Medicine*, vol. 41, no. 1, pp. 36–41, 2018.
- [18] J. Black, M. Barzy, D. Williams, and H. Ferguson, “Intact counterfactual emotion processing in autism spectrum disorder: evidence from eye-tracking,” *Autism Research*, vol. 12, no. 3, pp. 422–444, 2019.
- [19] P. Tashman, V. Marano, and J. Babin, “Firm-specific assets and the internationalization–performance relationship in the U.S. movie studio industry,” *International Business Review*, vol. 28, no. 4, pp. 785–795, 2019.
- [20] D. Stawarczyk, C. N. Wahlheim, J. A. Etzel, A. Z. Snyder, and J. M. Zacks, “Aging and the encoding of changes in events: the

- role of neural activity pattern reinstatement,” *Proceedings of the National Academy of Sciences*, vol. 117, no. 47, pp. 29346–29353, 2020.
- [21] L. C. Cheng and C. L. Huang, “Exploring contextual factors from consumer reviews affecting movie sales: an opinion mining approach,” *Electronic Commerce Research*, vol. 20, no. 4, pp. 807–832, 2020.
- [22] W. Xie, Z. Tian, Y. Zhang, H. Yu, and W. Ren, “Further studies on numerical instabilities of godunov-type schemes for strong shocks,” *Computers & Mathematics with Applications*, vol. 102, pp. 65–86, 2021.